Chinese Chemical Letters 37 (2026) 111676

Contents lists available at ScienceDirect

Chinese Chemical Letters

journal homepage: www.elsevier.com/locate/cclet

Slide ring polymer *in situ* cross-linked conductive ionogel for self-powered sensor

Yi Zhang[a,b], Yong Chen[a], Qian Wang[b], Jian-Qiu Li[a], Song-En Liu[a], Yu Liu[a,*]

[a] College of Chemistry, State Key Laboratory of Elemento-Organic Chemistry Nankai University, Tianjin 300071, China
[b] Tianjin Key Laboratory of Food Biotechnology, College of Biotechnology and Food Science, Department of Applied Chemistry, Tianjin University of Commerce, Tianjin 300134, China

ARTICLE INFO

Article history:
Received 29 March 2025
Revised 23 July 2025
Accepted 6 August 2025
Available online 7 August 2025

Keywords:
Supramolecular gel
Polyrotaxane
Cyclodextrin
Self-powered sensor

ABSTRACT

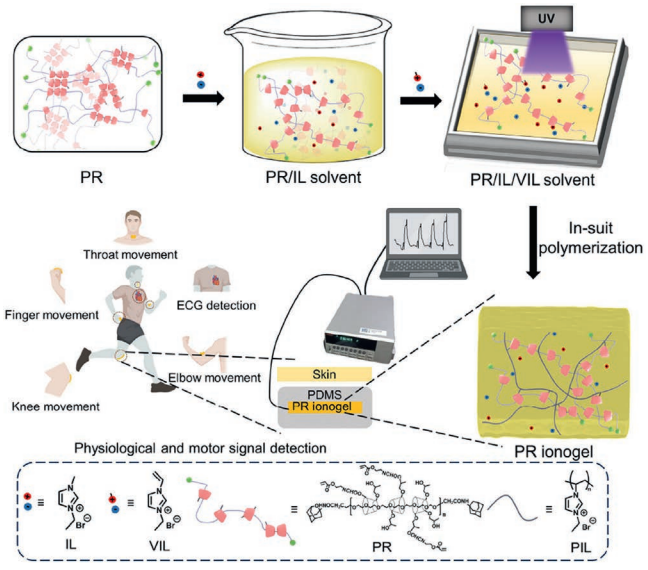
Possessing excellent mechanical properties, a high-coverage slide-ring conductive gel is constructed by *in situ* polymerization of α-cyclodextrin (α-CD) polyrotaxane (PR) and 1-vinyl-3-ethylimidazolium bromide ([VEIM]Br) ionic liquid (IL), using 1-ethyl-3-methylimidazolium bromide ([EMIM]Br) IL as solvent. Benefiting from the compatibility of ILs and alkene-PR, the cross-linked network slide-ring gel not only maintains excellent conductivity (1.52×10^{-2} S/m), but also has effectively improved mechanical properties (513 % fracture strain, 0.713 MPa fracture stress, 211 kPa elastic modulus and 1366 kJ/m^3 toughness) and adhesive properties (472.3 ± 25.9 kPa). The supramolecular gel can be used as a strain sensor to efficiently monitor deformation signals in real-time at least 200 times. Especially, the slide-ring gel can self-power generated by triboelectric effect and electrostatic induction between the skin layer and the polydimethylsiloxane (PDMS) layer that encapsulates the gel, achieving reversible and durable motion sensing, which provides a convenient pathway for constructing supramolecular self-powered flexible electronic materials.
© 2025 Published by Elsevier B.V. on behalf of Chinese Chemical Society and Institute of Materia Medica, Chinese Academy of Medical Sciences.

The rotaxane polymer network with the interlocking structure and high molecular mobility has attracted great attention from researchers in the field of supramolecular functional materials [1–4]. Polyrotaxane (PR), composed of α-cyclodextrin (α-CD) and polyethylene glycol (PEG), acts as the slide-ring cross-linking agent due to its unique topological structure and movement-generated pulley effect, which can effectively dissipate stress and endow the polymeric materials with excellent tensile properties and toughness [5,6]. As a result, rotaxane polymers have been widely used to construct stimuli-responsive materials [7,8], strain sensing materials [9], luminescent materials [10,11], adhesives [12,13] and bio-interfacial materials [14] to improve their mechanical properties and meet various application needs. For example, Bao *et al.* reported that PRs formed by poly(ethylene glycol methacrylate) sidechain functionalized α-CD thread PEG were introduced into the conductive polymer poly(3,4-ethylenedioxythiophene):poly(styrenesulfonate) (PEDOT:PSS) system and photo-crosslinked into a soft conductive membrane for surface-mounted and implanted electronic devices in living organisms [15], where the PR not only improves the mechanical properties of the film by sliding CD, but also enhances the conductivity by PEG-induced PEDOT aggregation. Liu's group reported that the highly stretchable supramolecular hydrogels were constructed by *in-situ* copolymerization of acrylamide with pseudopolyrotaxane cross-linker formed by double-bond modified PEG and α-CD, which were applied to stretchable supercapacitors and strain sensors [16,17]. However, in most PR polymer networks, the hydrogen bonding between CDs restricts the free sliding of the CD rings. Additionally, CD aggregation caused by hydrogen bonds impedes the free extension of the PR cross-linking agents within the polymer network. These effects ultimately impact the mechanical properties of the PR polymer. Ionic liquids (ILs) have been reported to effectively disrupt intermolecular hydrogen bonds and are excellent solvents for PR [18]. Jia's group introduced PR and IL into the polyacrylate cross-linking network to prepare a conductive ionogel with excellent mechanical properties. When compatible IL was introduced as dispersant, cyclodextrins on the rotaxane axle molecules had a high degree of sliding freedom, resulting in the ionogel having excellent tensile properties, fatigue resistance and low hysteresis. The ionogel was anticipated to establish a smart sensing system [19]. Therefore, ILs as solvents provide a convenient strategy for fabricating slide-ring conductive gels with high tensile strength and toughness.

On the other hand, ionogels constructed from IL with ionic conductivity and functionalizable properties are widely used in flexi-

* Corresponding author.
E-mail address: yuliu@nankai.edu.cn (Y. Liu).

https://doi.org/10.1016/j.cclet.2025.111676
1001-8417/© 2025 Published by Elsevier B.V. on behalf of Chinese Chemical Society and Institute of Materia Medica, Chinese Academy of Medical Sciences.



Scheme 1. Schematic illustration of the slide-ring ionogel for self-powered strain sensing.

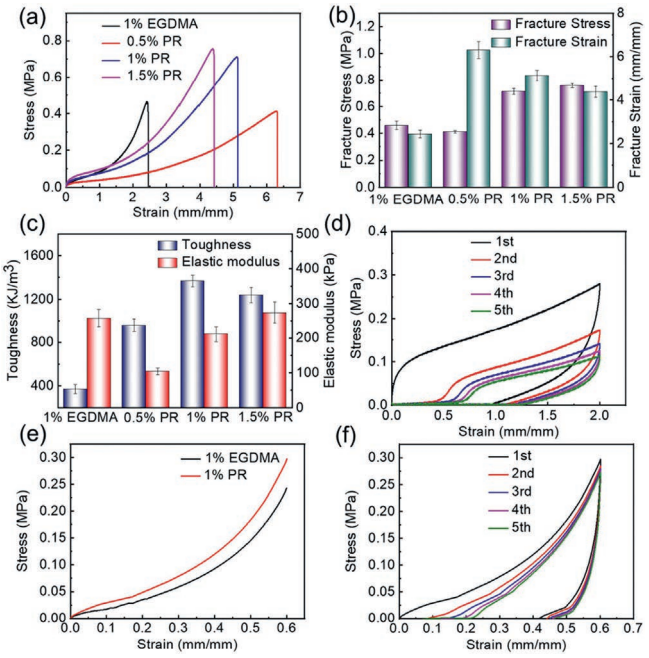


Fig. 1. Mechanical performances of ionogels. (a) Tensile stress-strain curves of ionogels with traditional cross-linkers and different ratios of PR cross-linkers. (b, c) The fracture stresses, fracture strains, elastic moduli, and toughness calculated from the stress-strain curves shown in Fig. 1a. (d) Tensile stress-strain cyclic hysteresis loops of 1PR-IG. (e) Compression stress-strain curves of ionogels with traditional cross-linkers and 1 % PR cross-linkers. (f) Compression stress-strain cyclic hysteresis loops of 1PR-IG.

ble sensors that can sense stimuli and transmit information [20], including various intelligent wearable devices [21], artificial skin [22,23], motion detection [24,25] and health management electronic devices [26–28]. Among them, triboelectric nanogenerators (TENGs) constructed from ionogels as electrode materials are ideal for sustainable, environmentally friendly, and safe power supplies for flexible wearable electronic devices because they can collect various forms of mechanical energy, including energy from human motion, and subsequently convert them into electrical energy. Although there have been some reports on the construction of gels from slide-ring polymers and IL, to the best of our knowledge, utilizing PR as a slide-ring crosslinking agent to prepare an ionogel for strain sensing and TENG self-powered materials is rarely reported. In the present work, the slide-ring ionogel is constructed by *in-situ* polymerization of 1-vinyl-3-ethylimidazolium bromide ([VEIM]Br) VIL and high-coverage PR in the solvent of 1-ethyl-3-methylimidazolium bromide ([EMIM]Br) IL, in which the slide-ring crosslinker PR is formed by acrylic ester modified α-CD threading PEG (Scheme 1). The good compatibility of PR crosslinker and [EMIM]Br enhances the sliding freedom of α-CD on the PEG chain, effectively improving the mechanical properties and adhesion properties of the ionogel and ensuring the conductivity of the ionogel to the maximum extent. Therefore, slide-ring conductive gel with high conductivity and excellent mechanical properties can be applied to sensitive and durable strain sensors, detection of human electrocardiogram (ECG) signals and TENGs for self-powered monitoring of human motion in real-time. The system promotes the development of self-powered gels and provides a new idea for macrocyclic supramolecular polymeric functional materials.

The PR crosslinker, formed by acrylic ester modified hydroxypropyl α-CD threading PEG chains and terminated with adamantane, was synthesized based on our previous report (~23 % CD coverage) [8]. The ionogel was constructed by dissolving PR crosslinker or traditional crosslinker ethylene glycol dimethacrylate (EGDMA) in IL solvent ([EMIM]Br), further mixing with IL polymerization monomer ([VEIM]Br), and *in-situ* polymerization under UV light. According to the FTIR before and after UV curing, the basic disappearance of the C=C bond vibration peak at 1660 cm^{-1} confirmed the occurrence of the polymerization reaction and the generation of poly(IL) (PIL) (Fig. S1 in Supporting information). A small amount of unreacted [VEIM]Br was dispersed in [EMIM]Br, which together acted as the solvent of the ionogel, and their good compatibility and electrostatic interactions with the PILs ensured that the gel had no IL leakage. Different ratios of PIL/IL crosslinked by a conventional crosslinker (EDGMA) allowed the formation of ionogels with extremely tunable mechanical properties. Tensile stress-strain results showed that the fracture strains of these gels were relatively low, but the mechanical strength increased in a wide range with the increase of PIL content (Fig. S2 in Supporting information). The increase in mechanical strength may be due to the large number of entangled PIL chains and the reduction of IL soft ionic domains. For the design of flexible electronic devices, the mechanical properties of the material are the primary consideration. The Young's modulus of those ionogels were 33.1 kPa (0.2 PIL/IL), 74.2 kPa (0.25 PIL/IL), 258 kPa (0.3 PIL/IL), 1.68 MPa (0.4 PIL/IL), 23.1 MPa (0.5 PIL/IL). Among them, the Young's moduli of 0.3 PIL/IL were relatively close to that of the skin [29,30], Therefore, 0.3 PIL/IL ionogel has a more suitable modulus range as a strain sensing material. Then, PR was introduced into 0.3 PIL/IL (containing 30 wt% PIL monomer) ionogel to improve its mechanical properties. The tensile stress-strain results of ionogels formed with different contents of crosslinkers were shown in Figs. 1a–c. As the PR content increased from 0.5 wt% to 1.5 wt%, the fracture stress of the ionogel increased from 0.412 MPa to 0.757 MPa, the elastic modulus increased from 104 kPa to 274 kPa, the toughness increased from 960 kJ/m^3 to 1238 kJ/m^3, and the fracture strain reduced from 630 % to 437 %. Compared to the mechanical properties (243 % fracture strain, 0.459 MPa fracture stress, 258 kPa elasticity modulus, and 370 kJ/m^3 toughness) of ionogel formed by conventional cross-linker EGDMA, the mechanical properties of PR ionogels were significantly improved. This is due to the good compatibility between PR and IL, which inhibits the aggregation caused by hydrogen bonding between CDs, so that the CDs on the slide-ring cross-linker in the ionogel can move freely on the PEG chain to the maximum extent and effectively dissipated energy through the pulley effect. The increase of PR content increased the cross-linking

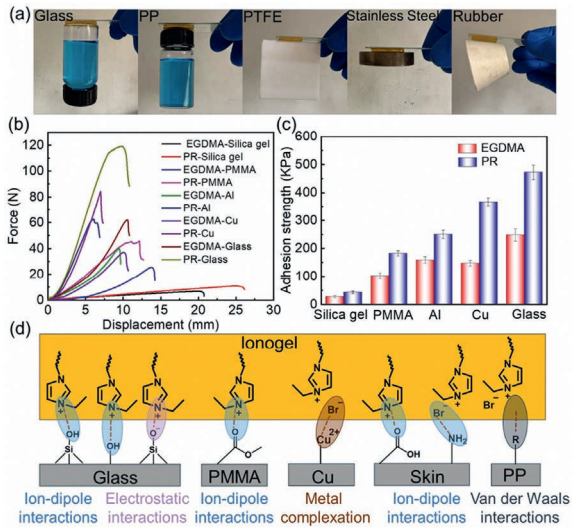


Fig. 2. (a) Photos of the adhesion of PR-IG to glass, PP, PTFE, stainless steel, and rubber. (b) Lap shear curve and (c) corresponding adhesion strength of 1PR-IG and traditional gel (1 % EGDMA) to silica gel, PMMA, Al, Cu and glass. (d) Possible adhesion mechanism of ionogel.

density of the network, which enhanced the toughness of the ionogel and decreased its elongation at break. Therefore, the ionogel containing 1 wt% PR (1PR-IG) showed the best comprehensive mechanical property parameters (513 % fracture strain, 0.713 MPa fracture stress, 211 kPa elastic modulus and 1366 kJ/m^3 toughness). The tensile stress-strain cyclic hysteresis loops of 1PR-IG under 200 % strain showed that it had a certain tensile reciprocating and fatigue resistance (Fig. 1d). The energy dissipation behavior of 1PR-IG was evaluated by continuous cyclic tensile loading-unloading experiments under different strains from 50 % to 400 % (Fig. S3 in Supporting information). The results showed that the slide-ring ionogel exhibited a large hysteresis loop. It can be calculated that as the strain increases, the dissipated energy gradually increases from 35.20 kJ/m^3 to 341.40 kJ/m^3, indicating that more dynamic ionic bond breakage occurs to dissipate energy with increasing strain. The results of the gels' compression experiments showed that both 1PR-IG and conventional ionogel could be compressed to 60 % strain of the original state without being destroyed. The compression stress of 1PR-IG reached 0.297 MPa, which was higher than 0.243 MPa of the conventional ionogel (Fig. 1e). After five reciprocal compressions of 1PR-IG (the compression strain was 60 %), the compression stress decreased from 0.297 MPa to 0.272 MPa, the gel strength did not decrease significantly, and the recovery rate of cyclic compression exceeded 91 % (Fig. 1f). These indicated that 1PR-IG had good compression and self-recovery properties. The good mechanical properties can also be seen from the photographs of 1PR-IG gel samples in tension and compression (Fig. S4 in Supporting information), which can be stretched up to 500 % of the original length without fracture, as well as compressed up to 60 % of the original height state to remain intact and basically recover after the stress is removed. All the above experimental results indicate that the supramolecular slide-ring ionogel has significantly enhanced mechanical properties, which are attributed to the slide-ring pulley effect of the PR crosslinker.

The adhesion properties of conductive soft materials are beneficial for their stable presence on the surface of the substance as well as the reduction of interfacial resistance. Excellent adhesion properties are very important for ionogel as a human motion sensor. As shown in the photo in Fig. 2a, 1PR-IG exhibited adhesion properties to glass, polypropylene (PP), polytetrafluoroethylene (PTFE), stainless steel, and rubber. This is because the ionogel 1PR-IG contains rich functional groups and electrons, which can achieve adhesion to different matrices through electrostatic interaction, ion-dipole interaction, metal complexation, van der Waals interaction, *etc.* (Fig. 2d). The adhesion strength of the ionogels was further characterised by lap shear adhesion tests (Fig. 2b). The lap shear curves results showed that the slide-ring ionogel and the conventional ionogel had adhesive effects on both the soft material silica gel, and the hard materials polymethylmethacrylate (PMMA) and glass, as well as metal materials copper (Cu) and aluminium (Al), with a maximum adhesion force of 119.1 N. Compared with the adhesion strengths of conventional ionogel to these materials in Fig. 2c (silica gel: 27.1 ± 3.8 kPa, PMMA: 101.9 ± 10.6 kPa, Al: 158.9 ± 11.7 kPa, Cu: 148.3 ± 10.2 kPa, and glass: 247.95 ± 22.1 kPa), 1PR-IG exhibited superior adhesion strengths (silica gel: 43.3 ± 5.2 kPa, PMMA: 183.0 ± 9.3 kPa, Al: 250.7 ± 15.4 kPa, Cu: 366.8 ± 14.2 kPa, glass: 472.3 ± 25.9 kPa). This may be due to the fact that supramolecular gel not only has multiple interactions to provide interfacial adhesion, but also in which the reversible sliding of the CD on the PEG chains can effectively dissipate the stresses that applied to the gel system, achieving nearly twice the improvement in adhesion performance. And the results of multiple adhesion tests on the glass substrate showed that the adhesion of 1PR-IG had decreased by 16 % after four times of repeated adhesion, which proved that 1PR-IG had a good service life (Fig. S5 in Supporting information). Then we investigated the thermal stability of the ionogels. Both traditional ionogel and 1PR-IG had excellent thermal stability. The thermogravimetric results (Figs. S6 and S7 in Supporting information) showed that the ionogels were stable below 250 °C under nitrogen condition with almost no weight loss. The rate of mass loss reached a maximum at temperatures up to 315 °C, at which point the mass of the ionogel decreased dramatically. The differential scanning calorimetry curves (DSC) in Fig. S8 (Supporting information) showed that the glass transition temperature (T_g) of the traditional gel was −41 °C. The 1PR-IG exhibited a much lower T_g (−61.76 °C). The lower T_g demonstrates that the introduction of PR improves the flexibility of the polymer system and reduces the resistance to the movement of the molecular chains, which is consistent with the improved mechanical and adhesion properties exhibited by the slide-ring gels. The X-ray diffraction (XRD) results (Fig. S9 in Supporting information) of 1PR-IG and the traditional gel showed that they had amorphous structures. Both slide-ring cross-linker and traditional cross-linker had good compatibility with IL, suggesting that CDs on PR were in a relatively free conformation in IL without the crystalline structure. The ^{1}H NMR spectrum showed that in the presence of [VEIM]Br IL, the chemical shifts of the 2-OH and 3-OH groups of CDs exhibited the upfield shift. This may be due to the hydrogen bonding of CD being disrupted in IL (Fig. S10 in Supporting information). In addition, AFM image further confirmed that there was no phase separation in the ionogel (Fig. S11 in Supporting information), that is, no cyclodextrin aggregation was observed, indicating that the IL destroyed the hydrogen bond induced CD aggregation. These inferences are consistent with previously reported literature [19]. Scanning electron microscopy (SEM) images showed that the gels had a dense structure (Fig. S12 in Supporting information), which was conducive to electron transfer and achieved high conductivity.

Conductivity, as another important property of ionogel, determines the application range of the materials in flexible electronics. First, 1PR-IG was connected in series to the circuit as an electronic component (Fig. S13 in Supporting information), whose conductivity successfully lighted up the light-emitting diode (LED). Moreover, the brightness of the LED decreased significantly with the 1PR-IG tensile strain increased. After cutting the 1PR-IG, the circuit was in a disconnected state and the LED did not light up. When the two cut parts were re-contacted, the LED was re-lighted with no significant difference from the original brightness, indicating that

the conductivity of the gel before and after cutting remained basically unchanged. The conductivity of the gels was investigated and calculated by the equation $\sigma = L/(R \times S)$, where R is the resistance of the ionogel as measured by electrochemical impedance spectroscopy. L and S are the length and cross-sectional area of the gel sample, respectively. Fig. S14 (Supporting information) showed that the conventional ionogel had a resistance of 1492 Ω and its conductivity was 1.34×10^{-2} S/m. The resistances of slide-ring ionogels with different PR contents were 1946 Ω (0.5 wt% PR), 1403 Ω (1 wt% PR), and 1319 Ω (1.5 wt% PR) respectively, corresponding to conductivities of 1.03×10^{-2}, 1.43×10^{-2} and 1.52×10^{-2} S/m respectively. The ionogel system had good electrical conductivity, and the introduction of PR maintained the electrical conductivity of the gel. The conductivity of these ionogels can meet the requirements of flexible electronic devices, which provides an experimental basis for their applications in strain sensors and TENGs.

The supramolecular gels with excellent mechanical and adhesion properties are ideal materials to construct flexible strain sensors. 1PR-IG with the best comprehensive performance was selected as the flexible sensor material to respond to strain, and the relative resistance change ($\Delta R/R$) process of the slide-ring ionogel with strain was tested. As shown in Fig. S15 (Supporting information), the $\Delta R/R$ of 1PR-IG exhibited an obvious increasing trend with the strain increase from 20% to 100%, and the gel's resistance can be kept stable at a fixed strain (Fig. S15a). When the strain of 1PR-IG was continuously stepped increased from 0% to 100% and then gradually recovered to 0% (Fig. S15b), the $\Delta R/R$ varied with the different strains, and it remained stable under the same stretch/release strain. These demonstrated that the ionogel was sensitive and stable to strain response. The 1PR-IG strain sensor demonstrated reliable $\Delta R/R$ changes during 10 cycles under three different strains of 20%, 50% and 100% (Fig. 3a). Even under large strains such as 150%, 300%, and 450%, the resistance changes remained stable during 10 reciprocating cycles (Fig. S15c). In addition, the $\Delta R/R$ exhibited a repeated decrease and recovery when the 1PR-IG was pressed multiple times (Fig. 3b). These experimental results further illustrated the stability and repeatability of the gel in strain responses. In order to investigate the durability of 1PR-IG strain sensors, the continuous stretch-release test was performed for 200 cycles at 100% strain, as shown in Fig. 3g, the strain sensors exhibited excellent electrochemical signal stability under 200 times reciprocal stretching, suggesting that the gel maintained structural integrity and strain sensitivity under this condition. The stability and reproducibility of 1PR-IG's strain response demonstrate that the supramolecular material is suitable for application in flexible strain sensors. Therefore, the 1PR-IG can be pasted onto the skin or clothing to realize real-time monitoring of human motion. To evaluate the performance of 1PR-IG as a wearable strain sensor, human motion detection experiments were conducted by attaching it to the fingers, wrists, elbows, knees, and throats, respectively (Figs. 3c–f and Fig. S16 in Supporting information). The results showed that when the finger, wrist, elbow, and knee joints bend, the $\Delta R/R$ of the ionogel increased and changed synchronously with the periodic bending of the joints. And the resistance showed different changes for different joint motions. In addition to large joint motion, the strain sensor can also detect small movements such as the swallowing of saliva. As shown in Fig. 3f, when the 1PR-IG was attached to the throat for swallowing movements, the change of $\Delta R/R$ clearly reflected this physiological activity. During the repeated cyclic motion process, the output electrical signals were basically the same, proving the stability and accuracy of the wearable strain sensor for motion detection. More importantly, the 1PR-IG can be used as a conductive electrode to detect real-time human ECG signals. After replacing commercial electrodes with 1PR-IG electrodes as shown in Fig. 3h, the ECG signal can be wirelessly transmitted to a personal computer for real-time display, the apparently separated P wave, QRS (Q-, R- and S-wave) complex wave and T wave of the human heartbeat were accurately measured, and multiple heartbeat waveforms were stably detected. These experimental results indicated that the slide-ring ionogel had application value in the field of wearable strain sensors and ECG signal detection. Considering the influence of sweat on 1PR-IG as a strain sensing material, we studied the mechanical properties and conductivity of 1PR-IG in the presence of different masses of artificial sweat (mainly including water and salts), and the results showed that the tensile properties and conductivity of

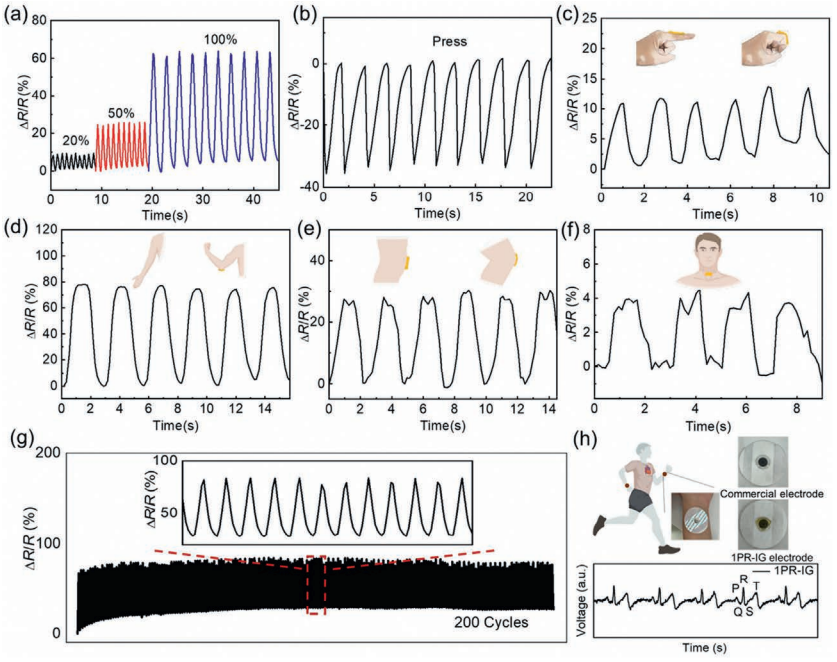


Fig. 3. (a) Reciprocating $\Delta R/R$ changes of 1PR-IG strain sensor under different strains (20%, 50% and 100%). (b) $\Delta R/R$ changes of 1PR-IG strain sensor under reciprocating compression. $\Delta R/R$ changes of 1PR-IG wearable strain sensor during (c) finger bending, (d) elbow bending, (e) knee bending, and (f) throat movement. (g) $\Delta R/R$ changes of 1PR-IG strain sensor under 100% strain and 200 consecutive tensile-release cycles. (h) 1PR-IG conductive electrode for real-time detection of human ECG signals.

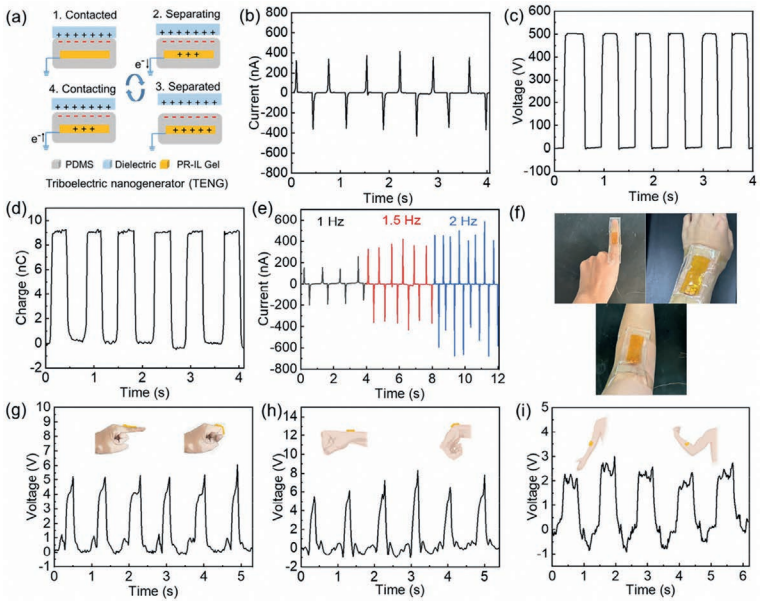


Fig. 4. (a) Schematic illustration of the working mechanism of PDMS/1PR-IG triboelectric nanogenerator. (b) I_{sc}; (c) V_{oc}; (d) Q_{sc} of the TENG at a frequency of 1.5 Hz. (e) I_{sc} of the TENG at different frequencies. (f) Photos of the PDMS/1PR-IG TENG as self-powered sensors attached to different joints of finger, wrist, and elbow. The V_{oc} signals of PDMS/1PR-IG TENG on the motion of (g) finger, (h) wrist, (i) elbow.

the gel were improved, but the toughness was reduced (Fig. S17a in Supporting information). This may be due to the weakening of ion-ion interactions in ionogel by polar solvent water, resulting in a decrease in electrostatic crosslinking density. The increase of gel conductivity may be attributed to the increase of free ions derived from salts in the system (Fig. S17b in Supporting information). Although sweat has a certain impact on the performance of gel, we effectively avoid the impact of sweat by encapsulating 1PR-IG within PDMS to form TENG as a self-powered strain sensor.

TENG are functional materials that convert mechanical energy into electrical energy by the triboelectric effect and electrostatic induction, which can be applied to wearable electronic devices [31,32] as well as health and motion detectors [33–35]. Here, a flexible self-powered TENG (PDMS/1PR-IG) with a sandwich structure was constructed by placing 1PR-IG between two layers of PDMS, where 1PR-IG acted as an electrode for charge transfer through an external connection to a copper wire (Fig. 4a). The working mechanism is as follows: when the dielectric material very high bond (VHB) contacts PDMS, the equal number of opposite charges are generated (the VHB surface with relatively low electronegativity is positively charged, while the PDMS surface with relatively high electronegativity is negatively charged). When the VHB is separated from the PDMS, the static charge of the PDMS causes the charge movement in the 1PR-IG, resulting in the formation of positive charges at the gel interface. At the same time, the double electric layer formed at the interface between the copper wire and the ionogel is polarized, and negative charges can be formed at the interface. The electrons in the copper wire will flow to the ground until the entire PDMS/1PR-IG reaches charge balance. When the VHB contacts the PDMS again, the whole process is reversed, and electrons can be transferred from the ground to the 1PR-IG electrode through the copper wire. Therefore, alternating current is generated by repeated contact-separation. To measure the electrical performance of PDMS/1PR-IG, we conducted contact separation movements of VHB and PDMS/1PR-IG at a frequency of approximately 1.5 Hz. As shown in Figs. 4b–d, the results showed that the open-circuit voltage (V_{oc}), the peak values of the short-circuit current (I_{sc}), and the transfer charge (Q_{sc}) of the TENG were 495 V, 338 nA, and 9.0 nC, respectively, indicating that it had good electrical signal output. Then, the effect of different friction frequencies on the output electrical signals was investigated. When the friction frequency was varied from 1 Hz to 2 Hz, the I_{sc} increased significantly with increasing frequency (from 152 nA to 454 nA) as shown in Fig. 4e, and the V_{oc} and Q_{sc} remained almost unchanged staying at 495 V and 9.0 nC (Figs. S18–S20 in Supporting information). This is because the change in frequency only affects the charge transfer rate, while the effective contact area between the friction layers remains constant. And the V_{oc}, I_{sc}, and Q_{sc} values remained almost the same in multiple cycles, proving the highly stable electrical output performance of the triboelectric nanogenerator. More importantly, the slide-ring gel TENG can be used as a self-powered biomechanical sensor to detect various human motions in real-time (Fig. S21 in Supporting information). Then, the TENG was fixed with tape on the fingers, wrists, elbows, and knees of humans to achieve self-powered (Fig. 4f), *i.e.*, skin instead of the VHB for contact-separation movement with the PDMS/1PR-IG. Due to the change in contact area between the generator and the skin during joint bending motion, the PDMS/1PR-IG exhibited significant voltage signals during the finger, wrist, elbow, and knee joint motion, and the V_{oc} value remained relatively stable (Figs. 4g-i and Fig. S22 in Supporting information). The bending motion of the knee was also reflected in the changes in I_{sc} and Q_{sc} values (Figs. S23 and S24 in Supporting information). And the outputs of these electrical signals had stability and sensitivity. This proves that the slide-ring ionogel TENG can convert the mechanical energy of human motion into electrical energy, and output electrical signals to achieve self-powered strain sensing. Table S1 (Supporting information) compared the mechanical, conductivity properties, and TENG output signal of this work with the reported gel materials. The results indicate that the performance of 1PR-IG and PDMS/1PR-IG TENG is comparable to or even better than previously reported gels. Therefore, 1PR-IG with good stretchability, conductivity, and adhesion can be applied to wearable self-powered strain sensors.

In summary, the slide-ring gels with high electrical conductivity and adhesion were constructed by *in-situ* copolymerization with IL monomer [VEIM]Br in IL solvent [EMIM]Br, using PR formed by acrylate-modified CD threading PEG as a sliding-ring cross-linker. Benefiting from PR's good solubility and high degree of sliding freedom in IL, the mechanical properties of the ionogels were ef-

fectively improved. The slide-ring gel with excellent mechanical and conductive properties can sensitively respond to external mechanical strains and display electrical signal changes, which can be used as a strain sensor to reflect human movement and detect human ECG signals in real-time. More importantly, the TENG constructed by the slide-ring ionogel has effective biomechanical energy harvesting and self-powered physiological activity monitoring. This study promotes the application of supramolecular functional materials for self-powered flexible wearable sensor materials.

Declaration of competing interest

The authors declare that they have no known competing financial interests or personal relationships that could have appeared to influence the work reported in this paper.

CRediT authorship contribution statement

Yi Zhang: Writing – original draft, Data curation, Conceptualization. **Yong Chen:** Writing – review & editing. **Qian Wang:** Writing – review & editing. **Jian-Qiu Li:** Data curation. **Song-En Liu:** Data curation. **Yu Liu:** Writing – review & editing, Conceptualization.

Acknowledgments

We thank National Natural Science Foundation of China (NSFC, No. 22131008), Natural Science Foundation of Tianjin (No. 22JCYBJC00500) and the Haihe Laboratory of Sustainable Chemical Transformations for financial support.

Supplementary materials

Supplementary material associated with this article can be found, in the online version, at doi:10.1016/j.cclet.2025.111676.

References

[1] J.S.W. Seale, Y.N. Feng, L. Feng, et al., Chem. Soc. Rev. 51 (2022) 8450–8475.
[2] Q.K. Cui, X.X. Zhang, Chin. J. Chem. 41 (2023) 2715–2729.
[3] L.Y. Chen, X.R. Sheng, G.F. Li, F.H. Huang, Chem. Soc. Rev. 51 (2022) 7046–7065.
[4] M. Tang, Z.R. Zhong, C.F. Ke, Chem. Soc. Rev. 52 (2023) 1614–1649.
[5] C. Liu, N. Morimoto, L. Jiang, et al., Science 372 (2021) 1078–1081.
[6] Y.Y. Wang, R. Shu, X.X. Zhang, Angew. Chem. Int. Ed. 62 (2023) e202303446.
[7] G. Bovone, E.A. Guzzi, S. Bernhard, et al., Adv. Mater. 34 (2022) 2106941.
[8] Y. Zhang, Y. Chen, H. Zhang, et al., Adv. Opt. Mater. 11 (2023) 2202828.
[9] X.R. Xiong, Y.H. Chen, Z.X. Wang, et al., Nat. Commun. 14 (2023) 1331.
[10] Y. Zhang, Y. Chen, J.Q. Li, et al., Adv. Sci. 11 (2024) 2307777.
[11] Y.H. Sun, L.N. Jiang, Y. Chen, Y. Liu, Chin. Chem. Lett. 35 (2024) 108644.
[12] S.H. Choi, T.W. Kwon, A. Coskun, J.W. Choi, Science 357 (2017) 279–283.
[13] K.V. Dikshit, A.M. Visal, F. Janssen, et al., ACS Appl. Mater. Interfaces 15 (2023) 17256–17267.
[14] J.Q. Yi, G.J. Zou, J.P. Huang, et al., Nature 624 (2023) 295–302.
[15] Y. Jiang, Z. Zhang, Y.X. Wang, et al., Science 375 (2022) 1411–1417.
[16] L. Feng, S.S. Jia, Y. Chen, Y. Liu, Chem. Eur. J. 26 (2020) 14080–14084.
[17] S.P. Wang, Y. Chen, Y.H. Sun, et al., Commun. Mater. 3 (2022) 2.
[18] S. Samitsu, J. Araki, T. Kataoka, K. Ito, J. Polym. Sci., Part B: Polym. Phys. 44 (2006) 1985–1994.
[19] R.C. Du, T.W. Bao, T.S. Zhu, et al., Adv. Funct. Mater. 33 (2023) 2212888.
[20] Z.H. Luo, W.J. Li, J.P. Yan, J. Sun, Adv. Funct. Mater. 32 (2022) 2203988.
[21] Y. Ding, J.J. Zhang, L. Chang, et al., Adv. Mater. 29 (2017) 1704253.
[22] D. Lv, X. Li, X. Huang, et al., Adv. Mater. 36 (2024) 2309821.
[23] T.Q. Li, Y.T. Wang, S.H. Li, et al., Adv. Mater. 32 (2020) 2002706.
[24] J.W. Wang, Y.P. Zheng, T.Y. Cui, et al., Adv. Funct. Mater. 34 (2024) 2312383.
[25] Q.M. Xia, W.Z. Li, X.Y. Zou, et al., Mater. Horiz. 9 (2022) 2881–2892.
[26] L.G. Xu, Z.K. Huang, Z.S. Deng, et al., Adv. Mater. 33 (2021) 2105306.
[27] M. Zhang, R. Yu, X. Tao, et al., Adv. Funct. Mater. 33 (2023) 2208083.
[28] Z.C. Yu, P.Y. Wu, Adv. Mater. 33 (2021) 2008479.
[29] Y. Li, N. Li, W. Liu, et al., Nat. Commun. 14 (2023) 4488.
[30] G. Du, Y. Shao, B. Luo, et al., Nano-Micro Lett. 16 (2024) 170.
[31] Q.Z. Sun, G.Z. Ren, S.H. He, et al., Adv. Mater. 36 (2024) 2307918.
[32] S.K. Fu, C.G. Hu, Adv. Funct. Mater. 34 (2024) 2308138.
[33] D. Yang, Y.F. Ni, X.X. Kong, et al., ACS Nano 15 (2021) 14653–14661.
[34] Y.X. Zhang, C.L. Xue, Y.P. Zhang, et al., Chin. Chem. Lett. 35 (2024) 109196.
[35] X.Y. Yu, W.J. An, L.N. Jiang, et al., ACS Appl. Mater. Interfaces 16 (2024) 68229–68236.